Hindawi
Advances in Civil Engineering
Volume 2021, Article ID 6613985, 12 pages
https://doi.org/10.1155/2021/6613985

Research Article

Improving the Stability of Subsurface Structures in Deep Metal Mines by Stress and Energy Adjustment: A Case Study

Huanxin Liu,[1,2,3] **Xingquan Liu**,[2,3] **Zhuoying Tan**,[1,4] **Yang Liu**,[2,3] **and Guilin Li**[2,3]

[1]*University of Science and Technology Beijing, Beijing 100083, China*
[2]*Deep Mining Laboratory of Shandong Gold Group, Laizhou, Shandong 261442, China*
[3]*Research Centre on Underground Non-Coal Mine Ground Pressure Disasters Prevention of Shandong Province, Laizhou, Shandong 261442, China*
[4]*Beijing Key Laboratory of Urban Underground Space Engineering, Beijing 100083, China*

Correspondence should be addressed to Zhuoying Tan; markzhy_tan@163.com

Received 20 November 2020; Revised 17 January 2021; Accepted 2 April 2021; Published 21 April 2021

Academic Editor: Arnaud Perrot

In deep hard-rock mines, the failure of subsurface structures (e.g., tunnels, stopes, and shafts) has been a significant problem affecting mining safety due to the high-stress environment. In this paper, the mechanism of structural failure and instability is discussed, and optimized excavation methods are proposed for stress control in deep gold mines. Based on the field observation and investigation of the joints distribution and rock failure modes at 800–1200 m depth of several large gold mines and a typical ultradeep borehole (2017 m depth) in northwest Jiaodong Peninsula, three engineering methods for reducing stress, including the stress transferring by mining optimizations, pressure relief by boreholes, and energy release in advance by optimizations of excavation and support, are analyzed by numerical simulation and field monitoring. Results show that stress reduction by excavation alone is limited and the backfill mining method is more conducive to stress transfer than the opening stope method. Roof contacted backfill can produce an unloading zone around the stope and reduce the stress of the surrounding stope. Relief boreholes can reduce the stress concentration of stopes, but the effect of cutting seams generated by presplitting blasting on pressure relief is not significant. The technology "short excavation and short support" releases less energy. By increasing the bench height and the reasonable timing of support by calculating, the elastic strain energy of rock in the shaft is prereleased, which benefits the long-term stability of the shaft.

1. Introduction

The excavation depth for metal mines worldwide has reached −1000 m to −2000 m, and the maximum mining depth is over −4000 m [1]. The in-situ stress for deep mines is normally high, which results in more and more mining/excavation-induced hazards, including rockburst, roof collapses, and shaft failure. It is well known that the excavation activities change the stress field of rock and the mining method, excavation order, and support time have effects on the stress change [2]. Therefore, some theoretical methods and practical technologies are proposed and developed to adjust the stress and energy in targeted areas, which improves the stability of rock mass in deep mines [3].

The stress state of the rock involves a series of complex formation processes [4–6], including the mechanical interactions between the exposed rock mass and the original rock, surrounding rock, and support system [7, 8]. In metal mines, considerable researches have been carried out to control the high-stress hazards. For example, Cai [9] established a mining design optimization and ground pressure control system. Wang [10] employed depressurization methods to maintain the development stability in high-stress areas. Ji et al. [11] developed a dynamic Coulomb failure stress increment model for quantitative assessment of the mining disturbance in high tectonic stress region and found that the disturbance effect in the working face perpendicular to a fault was much less than that parallel to the

fault. Therefore, a reasonable engineering layout is very helpful for reducing the risk of mining-induced risk. Feng et al. [12] summarized several methods to reduce the risk of rockburst, such as optimization of the excavation (or mining) size and sequences, high-stress aided blasting, boreholes to release energy, and advanced support system with the capacity of absorbing energy.

Moreover, the support method, time, and sequence could also affect the stability of deep rock mass. Kaiser and Cai [13] proposed a rock support design system under high stress and found that the bearing deformation capacity of rock bolts is an important parameter for reducing the risk of rockburst. Many rockburst supporting bolts were introduced. Besides, paste backfill technology has become an effective means to manage high stress and ground movement [14–16].

Although scholars have proposed many methods to control high-stress hazards of subsurface structures, there is a well-justified need to understand these methods in practice for rock engineering in deep mines. The deformation and failure of rock are affected by many factors, but the dominant factors are stress level and energy evolution. Therefore, it is of significance to adjust stress and energy for deep mining. This study is focused on employing some advanced engineering methods and practical management strategies for adjusting stress and energy in deep gold mines located in Jiaodong, China. First, key factors resulting in mining hazards and the control strategy are analyzed and discussed. The geological structures, failure characteristics of deep rock, and in situ stress field in the Jiaodong Peninsula are analyzed, observed, and measured. To reduce the risk of deep mining hazards, the engineering applications of stress transferring by mining optimizations, pressure relief by boreholes, and energy release by optimizations of excavation and support are studied by site monitoring and numerical simulations.

2. Deep Mining Hazard and Its Control Strategy

After the ore body has been excavated in deep hard-rock mines, the original stress balance is destroyed. The stress in the surrounding rock of subsurface structures is redistributed, and it reaches a new balance. Different zones, including concentration, release, and transformation of stress, are generated inside the surrounding rock. As a result, stress changes from three-dimensional to two-dimensional, making surrounding rock bear tensile stress. Once the stress exceeds the tensile strength or the compressive strength of rock mass, it causes joints and cracks to open or close [17, 18], leading to subsidence of stope roof, wedge caving, bottom swelling, spalling, slip, and even rockburst. All these phenomena are collectively known as ground behaviors caused by high stress [19].

The above analysis indicates that ground failures and instability are mainly affected by stress level, the structural plane of rock mass, and the mechanical properties of rock mass itself. High in-situ stress, especially tectonic stress, is necessary for rockburst [20], which is also the source of ground pressure in stopes and tunnels. In underground mines, many failures and instabilities could be attributed to the mechanical properties and the stress state of the rock mass, which is manifested as the contradiction between strength and stress:

$$K\sigma_v > S_c, \tag{1}$$

where K is the stress concentration factor; σ_v is the vertical component of original rock stress, MPa; and S_c is the rock strength, MPa.

Considering the effect of structure on rock strength, the above formula can be written as follows:

$$K\sigma_v > K_s S_c, \tag{2}$$

where K_s is the structure weakening factor.

From formula (1) and formula (2), it is noted that instability occurs when the stress level in rock mass exceeds its strength, especially along the structural plane.

Due to the difference in ore body shape, excavation (or mining) sequence, and mining methods, stress control becomes complicated in deep metal mines. The strategy for ground failure control can be summarized into four steps. Firstly, the tunnel's axis direction should be as parallel as possible to the maximum principal stress direction. The layout of some large subsurface structures such as chambers and shafts should avoid stress concentration areas, especially those areas near faults [21]. Secondly, transfer the secondary stress by optimization of excavation sequence and structure parameter, mining method innovation. Thirdly, pressure relief [22] and energy prereleasing technology are suggested to reduce stress concentration and form an unloaded zone. Finally, the surrounding rock mass can be reinforced by support components. Ground support requires that the support system be strong enough to sustain the momentum of the ejecting rock on the one hand and tough enough on the other hand to absorb the strain energies released from the rock mass [23]. So, it should adopt the flexible support for rock mass reinforcement which has the capacity of deformation and energy dissipation, such as flexible composite support, yield anchor, or cable to deform together with surrounding rock. The flexible support can not only control the stress but also prevent the further development of the structural plane in the rock mass. In summary, a control strategy and technical methods system for ground failure control is proposed in Figure 1.

3. Case Study

3.1. Background. The Jiaodong Peninsula of Shandong Province has many important metallogenic belts, such as the Zhaoyuan-Laizhou, the Qixia-Penglai, and the Muping-Rushan [24] (as shown in Figure 2). The three mainly developed ore-controlling fault zones are the Sanshandao-Cangshang fault (SSDF, see Figure 1), Xincheng-Jiaojia fault (JJF), and Zhaoyuan-Pingdu fault (ZPF). The types of gold deposits are mainly altered rock in fracture zones and quartz veins [25]. The lithology is dominated by a series of altered rocks, including sericite, serialized granite, serialized granitic

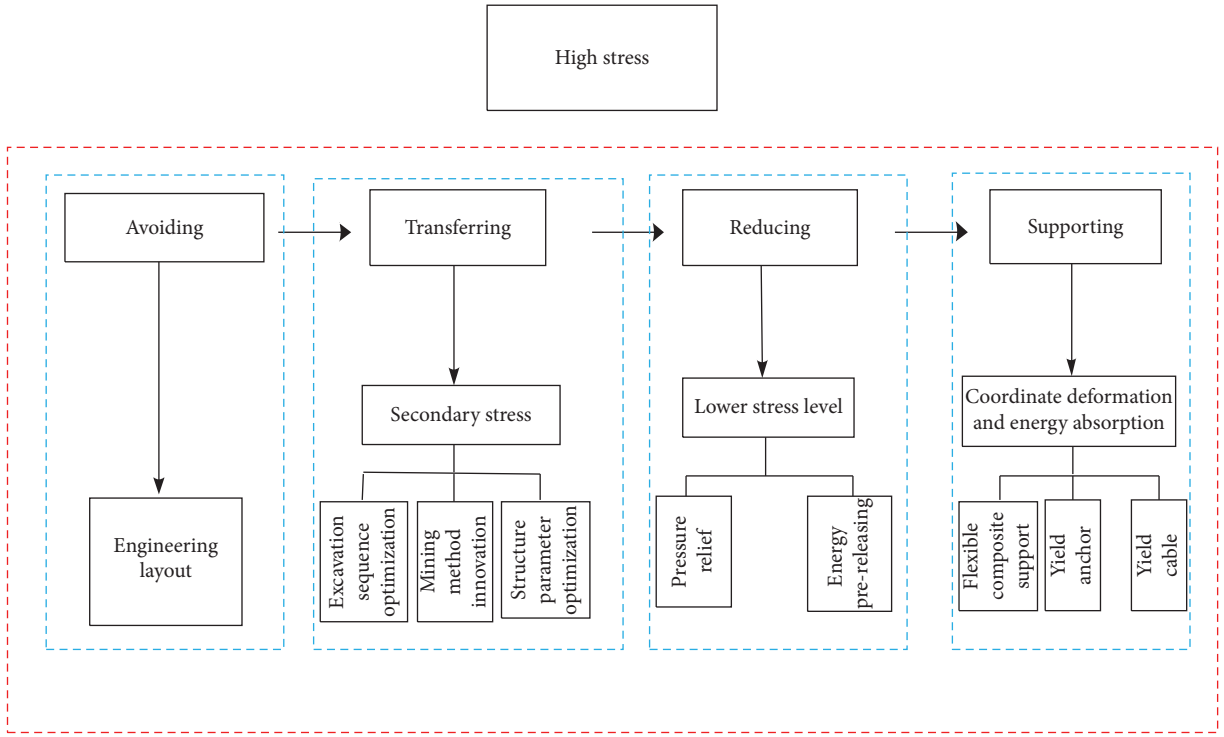

Figure 1: Strategy and system of technical methods for ground failures control.

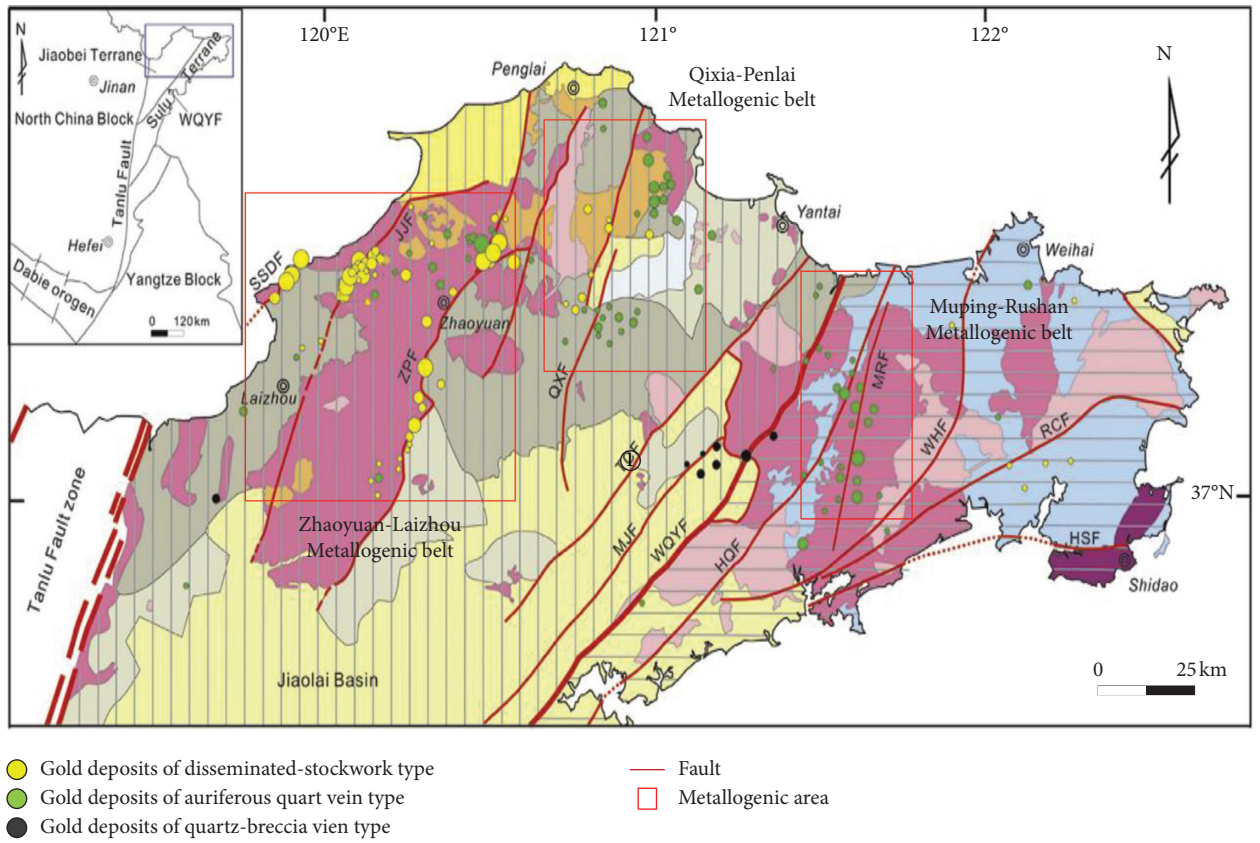

Figure 2: Distribution of faults and metallogenic belts in Jiaodong, China [24].

cataclastic, silicified granite, and potash for altered rock-type gold deposits granite.

Large and super-large gold deposits are mainly concentrated in northwestern Jiaodong [26]. The Zhao-Lai metallogenic belt has thousands of tons of gold resources, accounting for 80% of Shandong's gold reserves. Most metal mines' mining depth is below −800 m, and some mines with mining depths below −1000 m have experienced failures of the ground such as deformation of the tunnel, roof fall, and rockburst. So, it is very representative to choose this region as the research background.

3.1.1. Site Investigation. Our site investigation found that the rock mass joints and fractures were relatively developed in some deep stopes and tunnels, as shown in Figure 3.

Rock core disking phenomenon was found in some deep boreholes. Figure 3 shows the rock core from a 2017 m depth exploration hole in the Xiling mining area, Sanshandao Gold Mine at the levels of 1051.66–1056.40 m, 1088.96–1089.46 m, 1094.06–1097.06 m, 1467.76–1472.36 m, 1630.56–1632.36 m, 1761.36–1765.76 m, and 1765.76–1766.96 m. These observations indicate that the rock mass was under a high-stress environment, and tensile failures occurred (Figure 4).

Most mines investigations found slight or moderate rockburst phenomena at depths of −800 m to −1200 m, such as spalling rib and rock ejection, which caused a particular threat to mining construction and personnel safety. Some tunnels were severely deformed after a period of exposure. If the rock mass was broken, the tunnel roof would fall and exert a large force on support until it was completely failed, as shown in Figure 5.

3.1.2. Stress Level. Totally, 109 groups of in-situ stress measurement data were collected from 9 gold mines in northwestern Jiaodong [27–30] by stress-relief method, hydraulic fracturing method, and acoustic emission method, ranging from −71 m to −2300 m. It shows that the maximum horizontal principal stress in each group is more significant than principal vertical stress. Namely, horizontal stress is dominated by tectonic stress in this area. Measurement results show that $\sigma_{h,\max}$, $\sigma_{h,\min}$, and σ_v (MPa) increase almost linearly with depth, and the linear regression equations are as follows:

$$\sigma_H = 0.556H - 0.7772\left(R^2 = 0.8024\right), \quad (3)$$

$$\sigma_h = 0.0248H + 1.0504\left(R^2 = 0.8319\right), \quad (4)$$

$$\sigma_v = 0.0346H - 1.6137\left(R^2 = 0.9043\right), \quad (5)$$

where H is the depth (m) and R is the correlation coefficient. The variation of in situ stress with depth is shown in Figure 6. Correlation coefficients R^2 of the three principal stress fitting equations (formula (3) to formula (5)) are all greater than 0.8. It also indicates that the maximum horizontal principal stress distribution is relatively uniform and approximately 2.1 times vertical stress. At −1000 m depth, the maximum principal stress is up to 54.7 MPa.

Therefore, ground failures are mainly caused by high stress combined with a structure plane in northwestern Jiaodong at the current mining depth. The premise of control rock mass failures is to master the stress level and pay attention to the structure plane.

3.2. Stress Transferring. As mining advances, the stope's scale and shape change frequently, resulting in continuous secondary stress around the stope. The key of the stress transferring method is to transfer the stress of the stope to a nonmining area or surrounding rock.

In a mining area near the SSDF zone, mining depth has entered the −1050 m level, and the maximum horizontal principal stress is over 40 MPa. To ensure rock mass and improved ore production, two kinds of mining methods are designed: (1) the upward horizontal backfill method and (2) the approaching backfill method. A test stope is designed along the ore body strike, with a length of 60 m and a width of 40 m (average ore body thickness). To compare the total stress level of the two methods and the stress transferring process, a numerical simulation model with simulated mining depth ranges from −1050 m to −1005 m is developed in FLAC3D. In this model, the X-axis is perpendicular to the ore body strike, the Y-axis is along the ore body strike, and the Z-axis is along the plumb direction. It has a total of 1,188,000 elements, 1,231,466 nodes, and the 3D size is 240 m × 200 m × 45 m. The ore body has a dip angle of 40°, a fault called F1 is close to and almost parallel to the ore body, which is located in the hanging wall of the ore body, only about 40 cm thick, as shown in Figure 7. Physical and mechanical parameters for numerical simulation are shown in Table 1.

Table 2 shows two excavation schemes for optimizing the stress transferring effect [31]. The stress fields for the two exaction schemes are obtained by numerical simulations. In Scheme 1, as shown in Figure 8, if the stope is not filled, an unloading zone at the upper of the stope is formed after the excavation by Steps 1–3, and the reduction value of maximum stress about 7 MPa. However, the surrounding ore body's stress in two sides increases from 23.36 MPa to 25.59 MPa (Step 2), then reduced to the original level (Step 3). It can also be seen that a stress concentration zone is formed in the vault of stope in Step 1 and Step 2. Therefore, the stress reduction by excavation alone is limited. However, after backfilling without the roof contacted, the stress level in the backfill and the roof is reduced. The maximum principal stress is less than 2 MPa (Step 4), but the stress in the surrounding ore body is still high.

In Scheme 2, as shown in Figure 9, the roof and pillar stress has a slight reduction and the stress change in the surrounding ore body is not apparent in Step 1 and Step 2. After the first backfilling with the roof contacted (Step 3), an unloading zone is formed around the stope and it can also help reduce the stress in the pillars. In the subsequent excavation process, the stress around the stope and the filling body reduces to less than 2 MPa, and the stress value of the surrounding ore body also decreases to about 14.0 MPa (Step 4). After the final backfilling with the roof contacted,

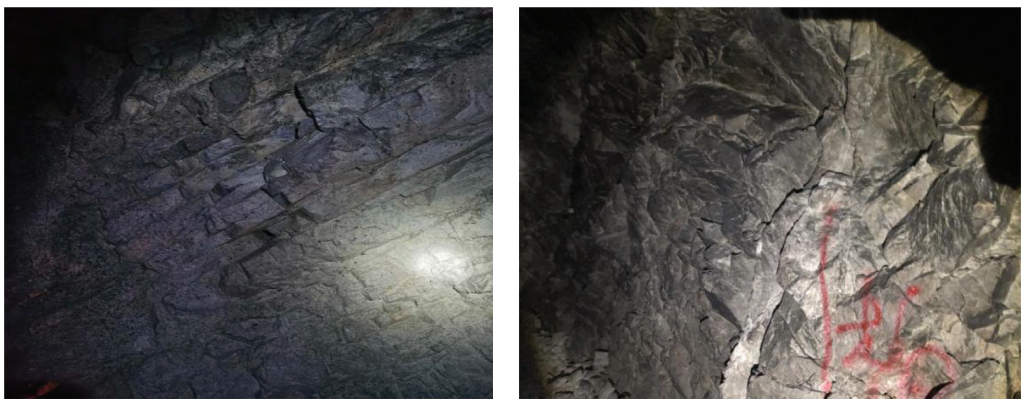

(a) (b)

Figure 3: Roadways with developed joints and fractures. (a) −1005m level, located at SSDF zone. (b) −815 m level, located at JJF zone.

Figure 4: Rock core disking phenomenon in an exploration hole with depth 2017 m.

(a) (b)

Figure 5: Continued.

(c) (d)

Figure 5: Typical ground failures in deep mining of northwestern Jiaodong. (a) Rockfall, −870 m level, located at SSDF zone. (b) Extruding deformation, −785 m level, located at MRF zone. (c) Rockburst, −980 m level, located at JJF zone. (d) Support failures, −1070 m level, located at ZPF zone.

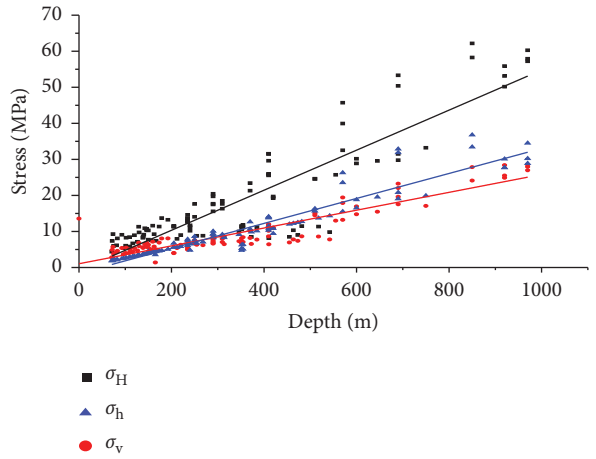

Figure 6: Relationship diagram of principal stress variations with depth in northwest Jiaodong.

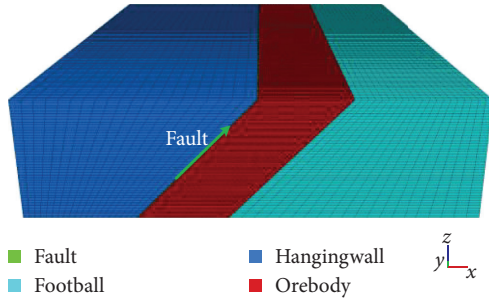

Figure 7: A 3D numerical model for mining-induced stress transferring.

the stress of the filling body is about 1 MPa. The stress of the surrounding ore body is significantly reduced.

Therefore, a better stress transferring effect can be obtained by Scheme 2, which not only can reduce the stress around the stope and filling body but also reduce the stress in the surrounding ore body. Scheme 2 can improve the stability of rock during mining and benefit the excavation of the adjacent stope.

3.3. Pressure Relief by Boreholes. During mining and tunnel construction, pressure relief holes can be drilled and blasted

Table 1: Physical and mechanical parameters for a numerical simulation model.

Location	Density (kg/m^3)	Bulk modulus (GPA)	Shear modulus (GPA)	Poisson's ratio	Cohesion (MPa)	Interfriction angle (°)	Compressive strength (MPa)	Tensile strength (MPa)
Hanging wall	2706	3.37	2.8	0.21	11.4	31.3	48.2	4.37
Football	2635	5.48	3.45	0.24	42.8	36.9	60.1	5.98
Fault	1925	0.595	0.378	0.26	0.128	18.4	20.6	0.0198
Ore body	2710	2.51	1.35	0.19	21.5	33.1	57.6	3.44
Filling body	1610	0.304	0.0245	0.17	0.261	35.6	7.43	0.212

Table 2: Designed mining schemes of test stope.

Mining method	Simulated mining scheme	Stress boundary
Scheme 1: the upward horizontal backfill method	Step 1: excavating an undercut roadway of 4 m × 4.5 m in the middle of a stope	Initial Szz −26.6 MPa
	Step 2: excavating north of stope	Initial Sxx −43.6 MPa
	Step 3: excavating south of stope	Initial Syy −26 MPa
	Step 4: backfilling height of 3 m with the roof uncontacted	
Scheme 2: the approaching backfill method	Step 1: excavating 4 approaching roads in the stope from the middle to the north	Initial Szz −26.6 MPa
	Step 2: excavating 3 approaching roads in the south of stope	Initial Sxx −43.6 MPa
	Step 3: backfilling the 7 roads with the roof contacted	Initial Syy −26 MPa
	Step 4: excavating the remained 8 roads	
	Step5: backfilling the 8 roads with the roof contacted	

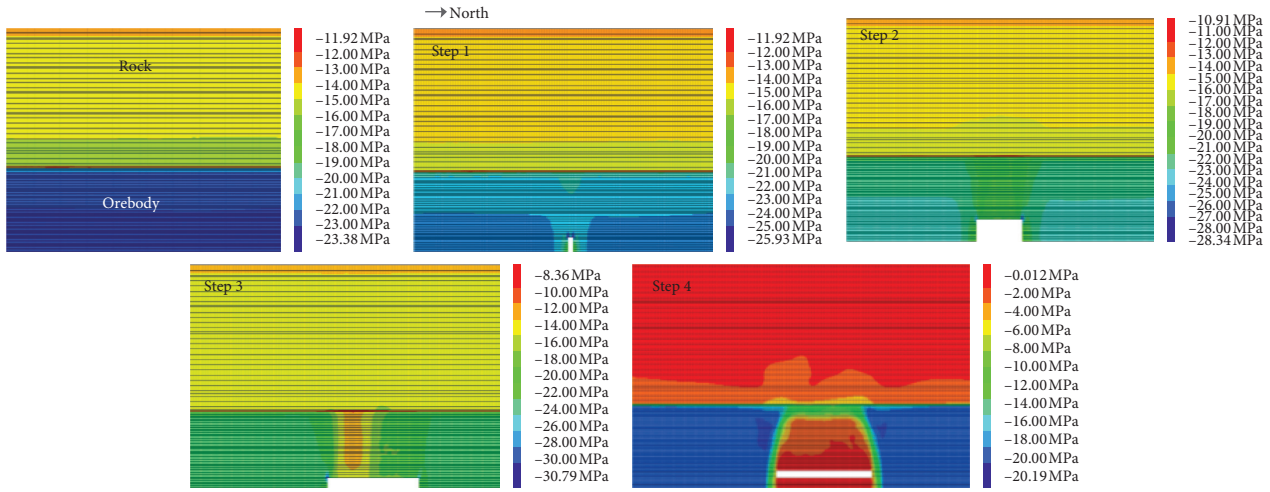

Figure 8: Stress transferring process of Scheme 1 (contour of maximum principal stress, $X = 70$ m).

in two sides or roof of the tunnel and stope to release the secondary stress caused by mining. A sublevel open stoping with subsequent backfill method is designed in −780 m level of a large gold mine located at SSDF zone, and a stope is chosen as industrial test stope. Before mining, a row of pressure relief holes is constructed in the adjacent drilling tunnel. The hole diameter is designed to be 65 mm, the bottom spacing between the two holes is 0.4 m, with a depth of 12 m. After the pressure relief holes are blasted, the area to be mined would be separated from adjacent areas by a connected cutting seam, which will help cut the mining disturbance stress transmission and form a local lower pressure zone.

As shown in Figure 10, an industrial stope is divided into three sections along strike: the south section, the middle section, and the north section. To compare stress-relief effect, different stress-relief measures are adopted in these three sections. The south section is to be mined without stress releasing holes. Stress-relief holes and presplit blasting are arranged in the middle section. Only pressure relief holes

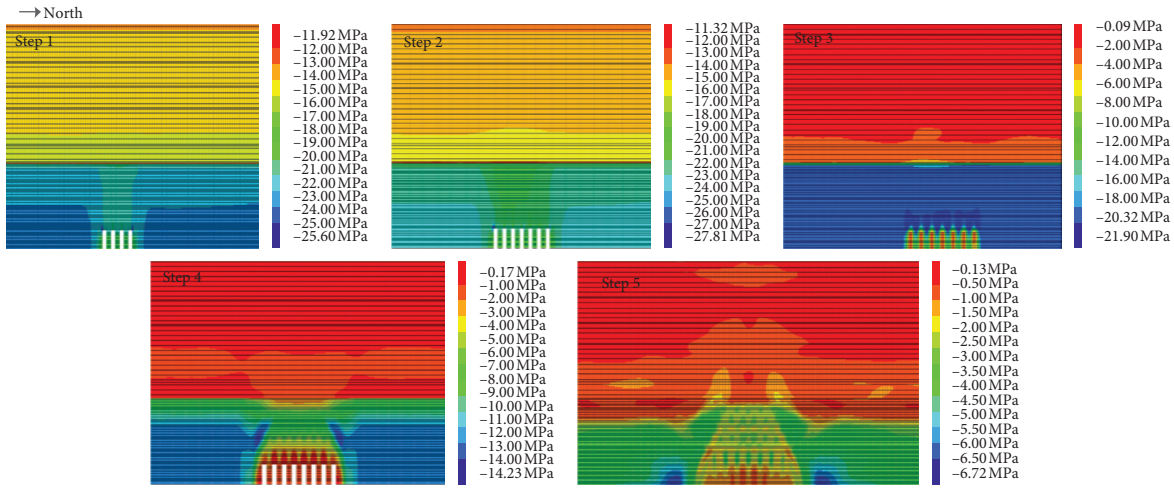

Figure 9: Stress transferring process of Scheme 2 (contour of maximum principal stress, $X = 70$ m).

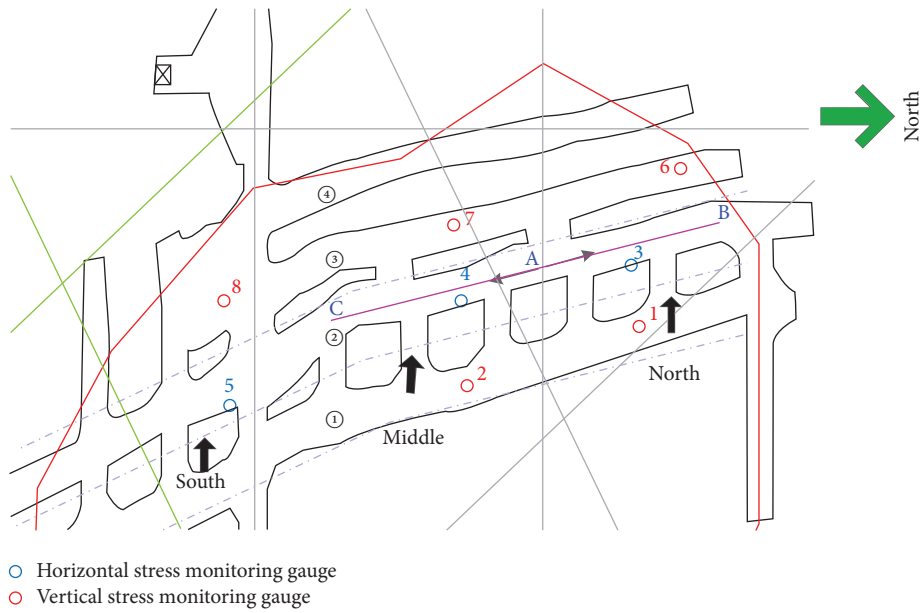

Figure 10: Layout of pressure relief holes and stress monitoring gauges.

are arranged in the north section and whether to conduct presplit blasting to form a cutting seam or not depends on stress relief in the middle section. The drilling process is started from center point A. Boreholes in section A-B are drilled first and those in section A-C are drilled later.

To obtain the pressure relief effect of boreholes and blasting, the stress values before and after the drilling and blasting are monitored. Eight borehole stress gauges are arranged in the south, middle, and north sections. The tracking monitoring is carried out for more than two months. The results are shown in Figure 11. The stress values of gauge #1, #2, #3, #6, and #7 are reduced to various degrees and tend to stabilize. Its average reduction is 23.80%, and the maximum reduction reached 37.56%. Nevertheless, there is an apparent increase in gauge #4, #5, and #8 and a followed sharp decline in gauge #5 and #8, due to later disturbance caused by mining activity in the South section. However, compared with the middle and north sections, the middle section's stress-relief effect is not better than the north section. Consequently, as a whole, it can reduce stress by proper bore drilling to maintain the stability of the stope, but the effect of presplit blasting is limited or need to be optimized.

3.4. Stress-Reducing by Energy Prereleasing. Rock excavation will inevitably lead to a large amount of elastic strain energy accumulated in the stress concentrated area. If energy accumulated in rock exceeds its capacity, instability or rockburst will occur [32]. The energy-releasing in advance technique requires a certain amount of time and space for energy-releasing before permanent shaft or tunnel support.

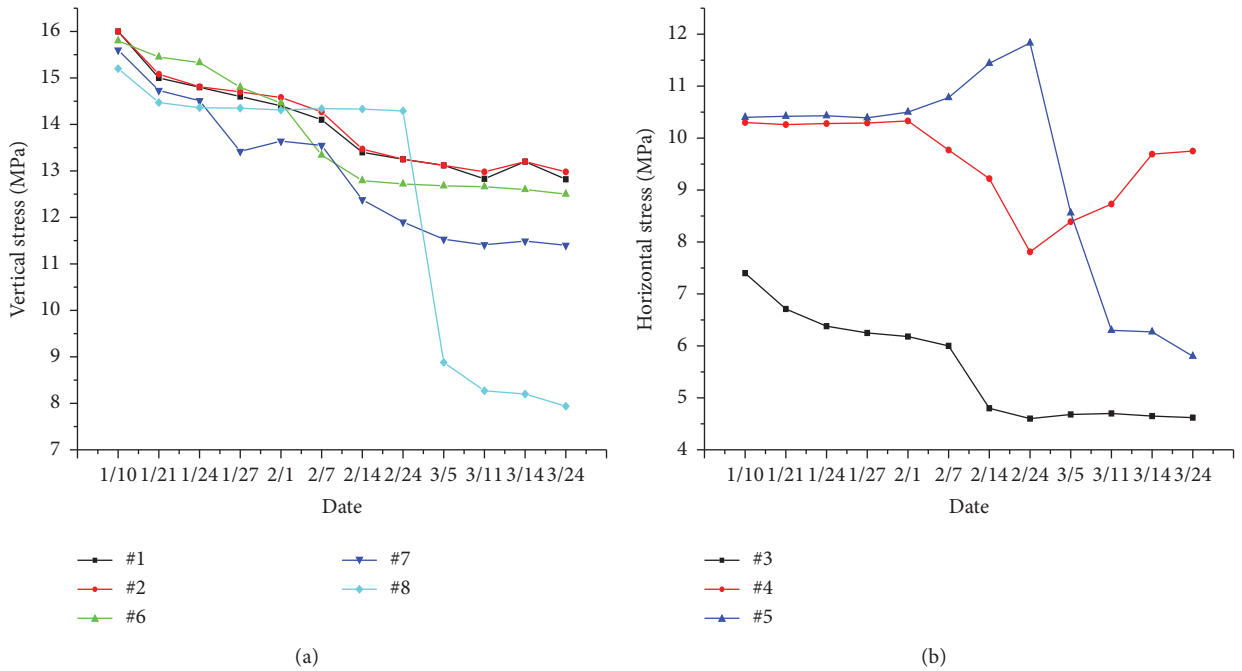

Figure 11: Stress curves of eight monitoring gauges: (a) vertical stress change curve and (b) horizontal stress change curve.

It is the surrounding rock rather than the permanent support to bear stress.

In a gold mine located at the JJF zone, a new main shaft has a designed diameter of 7.5 m and a net diameter of 6.7 m, with a total depth of 1527 m, from +32.9 m to −1494.1 m. After excavation, the stress in rock mass near-surface is redistributed, and a plastic failure zone would be produced. The tangential stress and radial stress in the plastic failure zone increased with increasing distance from the shaft center. It would increase to a much higher value than the in situ stress at the elastic-plastic interface.

A cross section of −1250 m level was selected as an example, where $P_0 = 38.96$ MPa, $c = 6.55$ MPa, $\varphi = 37.08^\circ$, and $a = 3.75$ m. The stress level and the plastic failure zone can be calculated by theoretical formulas (6)~(8) [33]. The result shows that $\sigma_\theta = 67.74$ MPa, $\sigma_r = 10.26$ MPa at the elastic-plastic interface, and $R_0 = 4.849$ m. It means the depth of the plastic zone is 1.10 m.

$$\sigma_r^{(p)} = (p_i + c\cot\varphi)\left(\frac{r}{a}\right)^{2\sin\varphi/(1-\sin\varphi)} - c\cot\varphi, \quad (6)$$

$$\sigma_\theta^{(p)} = (p_i + c\cot\varphi)\left(\frac{r}{a}\right)^{2\sin\varphi/(1-\sin\phi)}\frac{1+\sin\varphi}{1-\sin\varphi} - c\cot\varphi, \quad (7)$$

$$R_0 = a\left[\frac{(1-\sin\varphi)(p_0 + c\cot\varphi)}{p_i + c\cot\varphi}\right]^{(1-\sin\varphi)/2\sin\varphi}, \quad (8)$$

where $\sigma_r^{(P)}$ is the radial stress in the plastic zone, MPa; $\sigma_\theta^{(P)}$ is the tangential stress in the plastic zone, MPa; c is the cohesion, MPa; φ is the internal friction angel, °; P_i is the supporting reaction force, MPa; P_0 is the uniformly distributed in-situ stress, MPa; a is the radius of the shaft, m; r is the distance from the center of the shaft, and R_0 is the radius of the plastic zone, m.

Traditional construction process usually installs permanent support too early after a cycle (usually 4 m in China). However, it can be seen from the interaction model between surrounding rock and support, as shown in Figure 12, if we give the temporary support at time t_0 and give the permanent support at time t_1 (as support deformation characteristic curve 1), supporting material with higher stiffness is required. Besides, the permanent support may be damaged due to the high pressure on the support. If we give the temporary support at time t'_0 and give the permanent support at time t'_1 (as support deformation characteristic curve 2) on the premise of maintaining the stability of surrounding rock, it can not only ensure lining safety but also save support costs. Therefore, it is necessary to release energy accumulated in rock mass in advance to control stress effectively.

In this study, a construction section from elevation −930 m to −1271 m of 1527 m deep shaft is selected as the research object. Resin bolts and split set bolts with a particular ability to deform are selected as temporary supporting materials. Metal mesh and bimetal bars are selected to prevent the loose rock from slipping. The main functions of temporary support are to release dilatancy pressure and control loose confining pressure. According to rock mass rating (RMR) and geological strength index (GSI) classification results, the surrounding rock's stable height can reach 16~20 m without permanent support, as shown in Table 3. Besides, in Canada, a span of surrounding rocks without permanent support is suggested to be 2~3 times shaft diameter, and the corresponding construction time of this

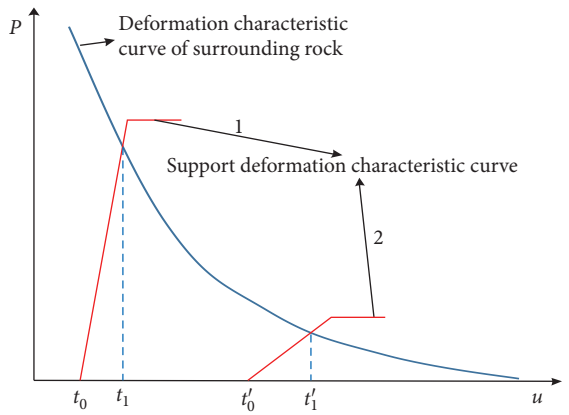

Figure 12: Interaction model between surrounding rock and support.

Table 3: Stable height calculation results based on the RMR evaluation.

Location (m)	RMR	Footage of advance (m)	Stable height (m)	Stand-up time (week)
−930~−972	69	4	20	>4
−972~−987	69	4	20	>4
−987~−1050	65	4	20	>4
−1050~−1073	65	4	17	>3
−1073~−1102	63	4	17	>3
−1102~−1153	69	4	16	>2
−1153~−1207	67	4	19	>4
−1207~−1250	69	4	20	>4
−1250~−1271	65	4	17	>3

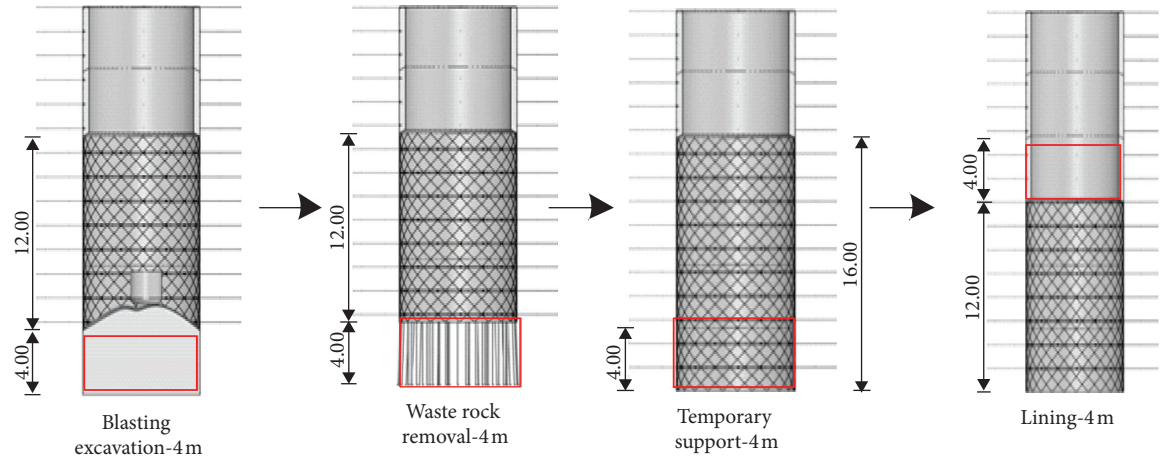

Figure 13: Construction process of the shaft using energy prereleasing techniques.

shaft is approximately 4~6 days. Therefore, the energy adjustment time of the new main shaft is determined to be 4 days, and the span of surrounding rock without permanent support immediately was 16 m (4 sinking cycle heights). The construction process can be shown in Figure 13.

To investigate stress change in surrounding rock and lining, a shaft model is established to analyze the maximum stress distribution in surrounding rock and concrete lining after improving the bench height without giving permanent support too early to release the energy in advance. Figure 14 shows that the maximum principal stress in the surrounding rock is reduced to less than 10 MPa in the range of 0~56 m from the working face, and most areas were close to zero. Similar variation patterns can be seen from the stress distribution in the concrete lining. The results show that improved technology can achieve a good stress control effect and create a lower pressure environment for the concrete lining.

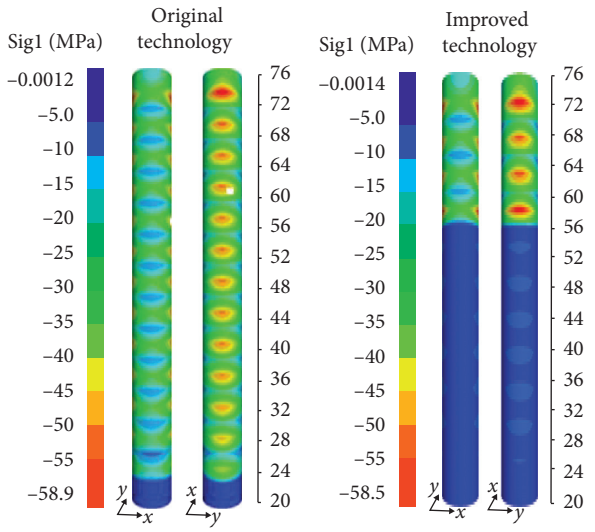

Figure 14: Longitudinal stress distribution in surrounding rock after adjusting construction technology.

4. Conclusions and Discussion

Through comprehensive geological investigation, field measurement, and in situ stress field analysis, the rock failure characteristics for deep gold mines in the Jiaodong area were obtained and adjusting stress and energy of excavated zone were determined as the main methods to improve the stability of subsurface engineering in deep mines. Conclusions can be given as follows:

(1) The maximum horizontal principal stress is the largest principal stress in the Jiaodong area, which indicates that the in situ stress field is dominated by horizontal tectonic movement. At −1000 m depth, the maximum principal stress is over 50 MPa. The ground failures are mainly caused by high stress.

(2) Compared with the open stoping method, the backfill mining method helps stress transfer, while the roof contacted backfilling is more conducive to stress transfer and failure control. An unloading zone around the stope can be produced by the roof contacted backfill method, which significantly reduces the stress level in the surrounding ore body.

(3) Pressure relief by boreholes and presplit blasting reveals that good-sized drilling boreholes can reduce stress. However, the effect of using presplit blasting to form a connected cutting seam on relieving pressure is limited.

(4) In deep shaft construction with a good rock mass quality, the traditional construction process of short excavation and lining early dissipates less energy. It may lead to support failures in a high-stress environment. Increasing the bench height without lining early and determining the proper support time is conducive to the energy prereleasing in the rock mass, which benefits the long-term stability of shaft construction and the reduction of support cost.

(5) In the future, it is suggested to carry out some research studies on how to utilize the high stress for rock breaking, which may reduce the use of explosives and control the ground failures effectively.

Data Availability

The data used to support the finding of this study are available from the corresponding author upon request.

Conflicts of Interest

The authors declare that they have no conflicts of interest.

Acknowledgments

This study was sponsored by the National Key Research and Development Projects of China (Grant no. 2018YFC0604601) and the Major Science and Technology Innovation Project of Shandong Province (Grant no. 2019SDZY05).

References

[1] H. Wu, G. Y. Zhao, P. Kulatilake, W. Z. Liang, and E. J. Wang, "Fracturing behaviour of sandstone specimens with a cavity formed by intersecting excavations under compression: experimental study and numerical modelling," *Strain*, vol. 55, no. 4, p. e12316, 2019.

[2] K. Xia, C. Chen, H. Fu, Y. Pan, and Y. Deng, "Mining-induced ground deformation in tectonic stress metal mines: a case study," *Engineering Geology*, vol. 210, pp. 212–230, 2016.

[3] C. C. Li, P. Mikula, B. Simser et al., "Discussions on rockburst and dynamic ground support in deep mines," *Journal of Rock Mechanics and Geotechnical Engineering*, vol. 11, no. 5, pp. 1110–1118, 2019.

[4] B. Orlecka-Sikora, "The role of static stress transfer in mining induced seismic events occurrence, a case study of the Rudana mine in the Legnica-Glogow Copper District in Poland," *Geophysical Journal International*, vol. 182, pp. 1087–1095, 2010.

[5] H. Wagner, "Deep mining: a rock engineering challenge," *Rock Mechanics and Rock Engineering*, vol. 52, no. 5, pp. 1417–1446, 2019.

[6] S. X. Wei, Y. Y. Wang, C. Y. Jin, L. B. Dong, and D. Liu, "Study on the ground settlement regularity caused by deep caving method," *Applied Mechanics and Materials*, vol. 670-671, pp. 907–911, 2014.

[7] X. Sun, C. Ren, J. Yuan, J. Du, J. Liu, and B. Guo, "The analysis of time-space effect of surrounding rock deformation of TBM tunnels in deep composite stratum with or without support," *Advances in Civil Engineering*, vol. 2020, Article ID 5494192, 21 pages, 2020.

[8] H. Zhang, J. C. Sun, X. C. Liu, M. Z. Gao, and S. G. Chen, "Analysis of deformation law of tunnel surrounding rock based on visualization of rock mass structure," in *Proceedings Of the 8th International Conference on Environment Science and Engineering*, Barcelona, Spain, March 2018.

[9] M. F. Cai, *Optimization of Mining Design and Ground Pressure Control in Metal Mines: Theory and Practice*, Science Press, Beijing, China, 2001.

[10] W. J. Wang, "Development working support method and practice in the high ground pressure mine," in *Proceedings Of*

the 7th International Symposium On Rock Burst And Seismicity In Mine, Dalian, China, August 2009.

[11] H. G. Ji, H. S. Ma, J. A. Wang, Y. H. Zhang, and H. Cao, "Mining disturbance effect and mining arrangements analysis of near-fault mining in high tectonic stress region," *Safety Science*, vol. 50, no. 4, pp. 649–654, 2012.

[12] X.-T. Feng, J. Liu, B. Chen, Y. Xiao, G. Feng, and F. Zhang, "Monitoring, warning, and control of rockburst in deep metal mines," *Engineering*, vol. 3, no. 4, pp. 538–545, 2017.

[13] P. K. Kaiser and M. Cai, "Design of rock support system under rockburst condition," *Journal of Rock Mechanics Geotechnical Engineering*, vol. 4, no. 2, pp. 215–227, 2012.

[14] N. Sivakuagan, R. M. Rankine, K. J. Rankine, and K. S. Rankine, "Geotechnical considerations in mine backfilling in Australia," *Journal of Cleaner Production*, vol. 14, no. 12-13, pp. 1168–1175, 2006.

[15] B. D. Thompson, W. F. Grabinsky, and W. F. Bawden, "In situ measurements of cemented paste backfill at the Cayeli Mine," *Canadian Geotechnical Journal*, vol. 49, no. 7, pp. 755–772, 2012.

[16] P. Y. Yang and L. Li, "Investigation of the short-term stress distribution in stopes and drifts backfilled with cemented paste backfill," *International Journal of Mining Science Technology*, vol. 25, no. 5, pp. 721–728, 2015.

[17] X. Xi, X. Wu, Q. Guo, and M. Cai, "Experimental investigation and numerical simulation on the crack initiation and propagation of rock with pre-existing cracks," *IEEE Access*, vol. 8, pp. 129636–129644, 2020.

[18] X. Xi, Z. Q. Yin, S. T. Yang, and C. Q. Li, "Using artificial neural network to predict the fracture properties of the interfacial transition zone of concrete at the meso-scale," *Engineering Fracture Mechanics*, vol. 242, p. 107488, 2021.

[19] B. Rahimi, M. Sharifzadeh, and X.-T. Feng, "Ground behaviour analysis, support system design and construction strategies in deep hard rock mining-justified in Western Australian's mines," *Journal of Rock Mechanics and Geotechnical Engineering*, vol. 12, no. 1, pp. 1–20, 2020.

[20] S.-J. Miao, M.-F. Cai, Q.-F. Guo, and Z.-J. Huang, "Rock burst prediction based on in-situ stress and energy accumulation theory," *International Journal of Rock Mechanics and Mining Sciences*, vol. 83, pp. 86–94, 2016.

[21] A. Iannacchione, T. Miller, G. Esterhuizen et al., "Evaluation of stress-control layout at the subtropolis mine, petersburg, Ohio," *International Journal of Mining Science and Technology*, vol. 30, no. 1, pp. 77–83, 2020.

[22] I. Vennes, H. Mitri, D. R. Chinnasane, and M. Yao, "Large-scale destress blasting for seismicity control in hard rock mines: a case study," *International Journal of Mining Science and Technology*, vol. 30, no. 2, pp. 141–149, 2020.

[23] H. Hu, H.-R. Liu, K. Yang, Y. Zuo, and Y. Cai, "Structural networks constraints on alteration and mineralization processes in the Jiaojia gold deposit, Jiaodong Peninsula, China," *Journal of Earth Science*, vol. 31, no. 3, pp. 500–513, 2020.

[24] X. F. Yu, D. P. Li, J. X. Tian, W. Shan, Z. S. Li, and P. F. Pei, "Gold metallogenisis and progress of deep exploration in Shandong Province," in *Proceedings Of the International Symposium On the Granulite Facies Metamorphism And the Early Plate Tectonics*, Laiyang, China, October 2018.

[25] L. Yang, J. Deng, R. Guo et al., "World-class Xincheng gold deposit: an example from the giant Jiaodong gold province," *Geoscience Frontiers*, vol. 7, no. 3, pp. 419–430, 2016.

[26] Z. J. Zhang, H. G. Ji, W. B. Wu, Y. Z. Zhang, and S. B. Jiang, "The research of rockburst hazards of Linglong gold mine base on the relationship of impact energy and confining pressure," *Applied Mechanics and Materials*, vol. 405-408, pp. 2391–2398, 2013.

[27] Z. S. Li, S. J. Miao, and F. H. Ren, "Research on comprehensive prediction of rock burst in Sanshandao gold mine," *Applied Mechanics and Materials*, vol. 170-173, pp. 1612–1617, 2012.

[28] H. X. Zheng, X. H. Zhang, T. H. Zhao, and X. H. Gao, "Geostress distribution and stress accumulation in Bohai Strait and adjacent area," *Chinese Journal of Rock Mechanics Engineering*, vol. 36, no. 2, pp. 357–369, 2017.

[29] C. D. Ma, Z. L. Liu, W. B. Xie, X. A. Wei, X. H. Zhao, and S. Long, "Comparative study of stress relief method and acoustic emission method in in-situ stress measurement in deep area of Xincheng Gold Mine," *Gold Science and Technology*, vol. 28, no. 3, pp. 401–410, 2020.

[30] M. F. Cai, J. A. Wang, and S. H. Wang, "Prediction of rock burst with deep mining excavation in linglong gold mine," *Journal of University of Science and Technology Beijing (English Edition)*, vol. 8, no. 4, pp. 241–243, 2001.

[31] C. Drover and E. Villaescusa, "A comparison of seismic response to conventional and face destress blasting during deep tunnel development," *Journal of Rock Mechanics and Geotechnical Engineering*, vol. 11, no. 5, pp. 965–978, 2019.

[32] S. Akdag, M. Karakus, G. D. Nguyen, A. Taheri, and T. Bruning, "evaLuation of the propensity of strain burst in brittle granite based on post-peak energy analysis," *Underground Space*, vol. 6, 2021.

[33] M. H. Yu, *Unified Strength Theory and its Application*, Xi'an Jiaotong University Press, Beijing, China, 2018.